Royal Astronomical Society

Downloaded from https://academic.oup.com/mnrasl/article/541/1/L28/8119388 by guest on 30 September 2025

MNRAS **541,** L28–L34 (2025) Advance Access publication 2025 April 24

Bridging the gap: OPTICAM reveals the hidden spin of the WZ Sge star GOTO 065054.49+593624.51

N. Castro Segura , 1,2* Z. A. Irving , 2 F. M. Vincentelli, 2 D. Altamirano, 2 Y. Tampo, 3,4 C. Knigge, 1 D. L. Coppejans, 1 N. Rawat, 3 A. Castro, 2,5 A. Sahu, 1 J. V. Hernández Santisteban, 6 M. Kimura, 7 M. Veresvarska, 8 R. Michel, 5 S. Scaringi, and M. R. Najera, 9

Accepted 2025 April 16. Received 2025 April 15; in original form 2025 January 21

ABSTRACT

WZ Sge stars are highly evolved accreting white dwarf systems (AWDs) exhibiting remarkably large amplitude outbursts (also known as superoutbursts), typically followed by short rebrightenings/echo outbursts. These systems have some of the lowest mass transfer rates among AWDs, making even low magnetic fields dynamically important. Such magnetic fields are often invoked to explain the phenomenology observed in these systems, such as their X-ray luminosity and long periods of quiescence (30+ yr). However, the detection of these is very elusive given the quenching of the accretion columns during outburst and the low luminosity of these systems during quiescence. Here, we present high-cadence multiband observations with OPtical TIming CAMera of the recent outburst of the recently discovered WZ Sge star GOTO 065054.49+593624.51, during the end of the main outburst and the dip in-between rebrightenings, covering two orders of magnitude in brightness. Our observations reveal the presence of a statistically significant signal with $P_{\omega} \simeq 148$ s in the bluer (g) band, which is detected only during the dip between the main outburst and the rebrightenings. We interpret this signal as the spin period of the AWD. If confirmed, GOTO 065054.49+593624.51 would bridge the gap between intermediate- and fast-rotating intermediate polars below the period gap.

Key words: accretion, accretion discs – stars: dwarf novae – stars: individual: GOTO 065054.49+593624.51.

1 INTRODUCTION

Cataclysmic variable stars (CVs) are binary systems in which a low-mass secondary star, filling its Roche lobe, transfers mass to a white dwarf (WD) primary. In systems where the magnetic field is dynamically unimportant, the accretion process is mediated by an accretion disc. If the magnetic field of the WD is sufficient to prevent the formation of the disc, this gives rise to the so-called *polars*. If, on the other hand, a disc can form but is truncated by the magnetosphere of the central WD, the systems are traditionally classified as *intermediate polars* (IPs); however, recent findings suggest that some IPs may be disc-less (e.g. Littlefield et al. 2021). Disc-mediated systems with mass transfer rates sufficiently low to prevent the disc from remaining persistently in a fully ionized state are classified as dwarf novae (DNe; see e.g. Warner 1995, for a review on CVs). DNe are characterized by exhibiting eruptions where the

WZ Sge systems are highly evolved short orbital period DNe, which exhibit even larger amplitude outbursts (up to \sim 8–9 mag). These so-called superoutbursts are characterized by prolonged outburst durations (approximately 30 d), and the appearance of superhumps – low-amplitude variations near the system's orbital period – shortly after reaching peak brightness (Smak 1993, 2009; Patterson et al. 2005; Kato 2015; Hameury 2020). These superoutbursts are typically followed by a series of short-term rebrightenings or echo outbursts, which seem to be characteristic of accreting binaries with extreme mass ratios. These rebrightenings cannot be explained by the standard disc instability model (e.g. Hameury 2020). To reconcile observations with theoretical predictions, Campana et al. (2018) recently proposed an alternative explanation where the luminosity drops during outburst decay signal a temporary transition to a

¹Department of Physics, University of Warwick, Gibbet Hill Road, Coventry CV4 7AL, UK

²Department of Physics & Astronomy, University of Southampton, Southampton SO17 1BJ, UK

³South African Astronomical Observatory, PO Box 9, Observatory 7935, Cape Town, South Africa

⁴Department of Astronomy, University of Cape Town, Private Bag X3, Rondebosch 7701, Cape Town, South Africa

⁵Instituto de Astronomía, Universidad Nacional Autónoma de México, Carretera Tijuana-Ensenada Km. 107, Ensenada, B.C. 22860, México

⁶SUPA School of Physics and Astronomy, University of St Andrews, North Haugh, St Andrews KY16 9SS, UK

⁷Advanced Research Center for Space Science and Technology, College of Science and Engineering, Kanazawa University, Kakuma, Kanazawa, Ishikawa 920-1192, Japan

⁸Centre for Extragalactic Astronomy, Department of Physics, Durham University, South Road, Durham DH1 3LE, UK

⁹NAF – Osservatorio Astronomico di Capodimonte, Salita Moiariello 16, I-80131 Naples, Italy

system brightens typically 2–5 mag for a relatively short period of time. Such eruptions are thought to be the consequence of a sudden increase in the mass accretion rate on to the compact object due to the accretion disc transitioning from a neutral to a fully ionized state (e.g. Lasota 2016).

^{*} E-mail: Noel.Castro-Segura@warwick.ac.uk

magnetic propeller state. This is an appealing framework as it could help to explain the behaviour of accreting systems at different scales, i.e. X-ray binaries, young stellar objects, and CVs. This framework also aligns well with the proposed spin period of 27.87 s of WZ Sge (Patterson 1980; Patterson et al. 1998). However, using Hubble Space Telescope time-resolved spectroscopy, Georganti et al. (2022) showed that WZ Sge does not exhibit any propeller footprint during the proposed propeller state (cf. Eracleous & Horne 1996). None the less, truncation of the inner disc is required to explain the relatively high X-ray luminosity. Against this background, Hameury (2020) proposed that the X-ray excess observed in WZ Sge could (also) be a consequence of evaporation of the inner disc, while the quiescent phases between outbursts are produced by overflows of the mass transfer stream impacting the inner regions of the disc, similar to what is proposed to explain IW And systems and some nova-like CVs (Kimura et al. 2020; Castro Segura et al. 2021). Regardless of whether magnetic fields are responsible for the X-ray luminosities in WZ Sge stars, they are often invoked to explain the very long recurrence time-scales in these systems (Kato 2015).

In this letter, we report high-cadence multiband photometry of the newly discovered transient GOTO 065054.49+593624.51 (hereafter GOTO 0650) obtained with OPtical TIming CAMera (OPTICAM; Castro et al. 2019, 2024). GOTO 0650 was discovered by the Gravitational-wave Optical Transient Observer (GOTO; Steeghs et al. 2022; Dyer et al. 2024) on 2024 October 4 03:36:36 UT (Killestein et al. 2024a). The transient reached an L-band ($\sim g + r$) magnitude of 13.7 in the discovery images and was associated with an ~22nd mag quiescent counterpart implying an outburst amplitude of \sim 8.5 mag, typical of WZ Sge stars. The nature of the transient was confirmed by spectroscopic observations and ultraviolet (UV) photometry (e.g. Bhattacharya & Bhattacharyya 2024; Killestein et al. 2024b). Using data from the American Association of Variable Star Observers (AAVSO 20242024) and the Zwicky Transient Facility (ZTF; Bellm et al. 2019a, b), we show in Fig. 1 how the outburst evolution and rebrightenings are consistent with the classification above. Tampo (2024) reported the onset of regular superhumps after a type-E recovery of a dip ~15 d from the beginning of the outburst (e.g. Kimura et al. 2018), and suggested that GOTO 0650 is a period bouncer with an orbital period close to the superhump period ($P_{\rm sh} = 91.05 \pm 3$ min), again, in line with GOTO 0650 being a member of the WZ Sge-type DNe.

2 OBSERVATIONS AND DATA REDUCTION

The OPTICAM (Castro et al. 2019, 2024) is a new high-cadence, multiband camera mounted on the 2.1-m telescope at the San Pedro Mártir Observatory (OAN-SPM), in México. OPTICAM is equipped with three Andor Zyla 4.2-Plus scientific Complementary Metal–Oxide–Semiconductor (sCMOS) cameras with three 2048 × 2048 pixels and a set of Sloan Digital Sky Survey (SDSS) filters (ugriz), allowing coverage in the range from 3200 Å to 1.1 μ m. The field of view is $\approx 5 \times 5$ arcmin² with a pixel scale of ≈ 0.15 arcsec pix⁻¹.

GOTO 0650 was observed in the g, r, and i bands during the nights of October 26, 28, and 30 and November 2 and 4 of 2024. The sky conditions were photometric for all the nights except for the last one, during which variable high clouds were present; this is reflected in our ability to recover the i-band photometry in Epoch 5. The details of the observations can be found in Table 1. The data were primarily reduced using version 1.13.0 of the PHOTUTILS PYTHON package (Bradley et al. 2024). Cosmic rays were clipped from all images using the Laplacian Cosmic Ray Identification (L.A.Cosmic) algorithm (van Dokkum 2001) as implemented in ASTRO-SCRAPPY

version 1.2.0 (McCully et al. 2018). For each image, two-dimensional background images were calculated using the SextractorBackground estimator from PHOTUTILS with a box_size of 64 pixels for 2×2 binning or 42 pixels for 3×3 binning. Image segmentation was used to identify sources in the background and subtracted images using the SourceFinder routine from PHOTUTILS, which combines source detection and deblending. To identify sources, we set the npixels parameter to 32 pixels for 2×2 binning and 14 pixels for 3×3 binning. The threshold parameter was set to $5 \times$ background RMS, and the background RMS was estimated using StdBackgroundRMS. All other parameters were left to their default values.

We used the optimal photometry algorithm described in Naylor (1998) to perform photometry on the background-subtracted images. We model the point spread function (PSF) of OPTICAM's three cameras using two-dimensional Gaussians for each camera. We stacked the images from each epoch for each camera to get the PSF parameters. We then identified sources in the stacked images using SourceFinder, which assigns a semimajor and semiminor standard deviation to each source. The PSF for each camera in each epoch was then modelled using the median semimajor and semiminor standard deviations from the corresponding stacked image. We then used differential photometry to correct for atmospheric variability; relative light curves were computed using the summed fluxes of the same (non-variable) reference stars in each night.

3 ANALYSIS AND RESULTS

The high-cadence photometric light curves are presented in the left panels of Figs 2 and 3; the comparison stars in these figures are always the same (namely Gaia EDR3 1003219393009879424 and 1003225264228638336), so the change in relative flux between epochs is meaningful. As can be seen in Fig. 1, Epochs 1 and 2 were taken towards the end of the superoutburst, Epoch 3 was taken during the decline, and Epochs 4 and 5 occurred during the dip between the main outburst structure and the rebrightenings, when the source was \sim 4–5 mag fainter than the first observation but \sim 3 mag brighter than the quiescent level. During Epochs 1–3, the source was dominated by the regular superhumps reported by Tampo (2024), with the dispersion in the light curves reducing as the accretion disc got fainter. In Epochs 4 and 5, there is still a slow modulation present with similar frequency as before, as can be seen in Fig. 3, the general trend is similar but the g band exhibits higher amplitude (than at least the r band). In both of these epochs, we can see short-term variability in the g band, suggesting the presence of an additional component contributing to the modulation of the light curve.

To characterize the short-term variability of GOTO 0650, we have computed the generalized Lomb-Scargle periodogram (LSP; Lomb 1976; Scargle 1982; VanderPlas 2018) for each light curve as implemented in ASTROPY version 6.1.2. We normalized our LSPs according to

$$P = 2\delta t P_{\rm LSP},\tag{1}$$

where δt is the time resolution of the light curve and $P_{\rm LSP}$ represents the *unnormalized* LSP powers. This normalization is defined such that the integrated periodogram yields the variance of the light curve¹ (Vaughan et al. 2003).

¹Provided the time series is uniformly sampled and the LSP is evaluated at the Fourier frequencies.

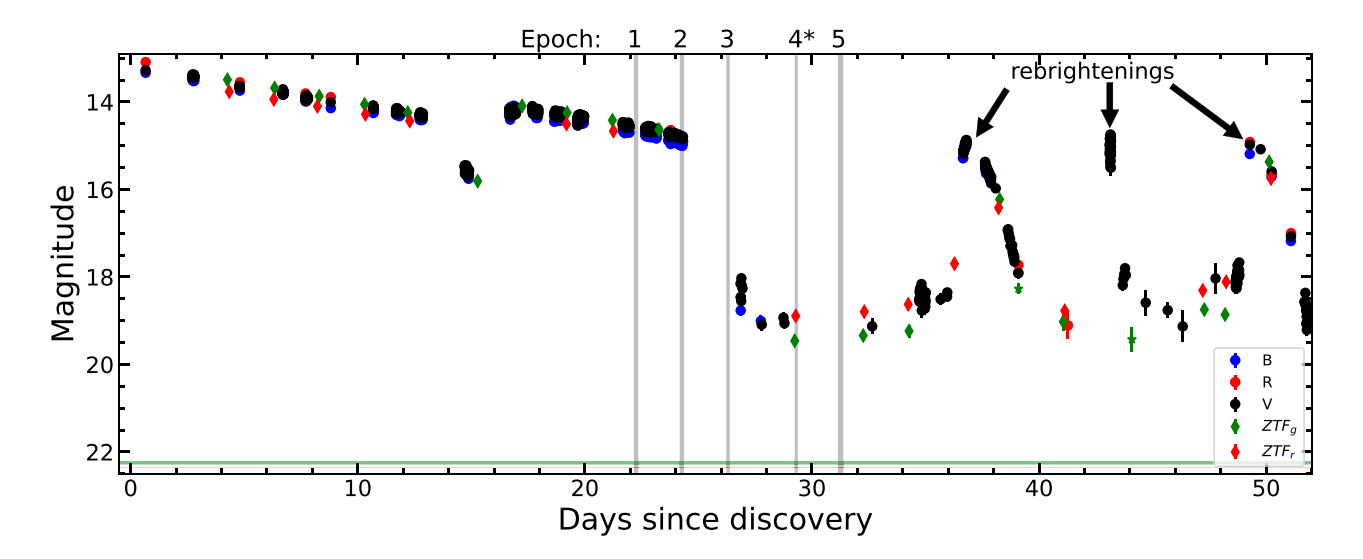


Figure 1. Outburst evolution of GOTO 0650 as reported by the AAVSO (circles) and ZTF (diamonds for PSF photometry and stars for forced photometry). The different colours indicate the magnitude in different bands. The coloured horizontal bands encompass the $\pm 1\sigma$ error around the weighted mean of the quiescent photometry obtained with forced photometry on ZTF during 9–25 d before the onset of the superoutburst; the precise values are $g = 22.25 \pm 0.03$ mag and $r = 22.351 \pm 0.005$ mag. The arrows highlight the maxima of the post-outburst rebrightening/flares. The time of the high-cadence observations with OPTICAM are indicated with the grey shaded regions, and the epoch ID for each observation reported in this letter is indicated on the top axis. (*) denotes the epoch with a statistically significant detection of the 148 s signal.

Table 1. Observing log. The star in the epoch number denotes statistically significant detection of short-term periodicity (see Section 3 for details).

Epoch	MJD _{start} (d)	Filters	Exposure time (s)	Obs. length (h)	Binning
1	60609.31	gri	3	4.65	2 × 2
2	60611.33	gri	3	4.54	2×2
3	60613.38	gri	5	3.62	2×2
4*	60616.39	gri	15	3.34	3×3
5	60618.29	gri	15	5.89	3×3

To estimate the confidence levels of the proposed signals in our LSPs, we model the continuum analytically following the method described in appendix A of Vaughan (2005), which we note is only applicable to the LSP if the time series is uniformly sampled and the LSP is evaluated at the Fourier frequencies (VanderPlas 2018). We compute confidence thresholds by scaling our continuum model by $-2\ln(\epsilon/n')$, where ϵ is the desired false alarm probability and n' is the number of LSP ordinates used to fit the model. The LSP for each of the light curves is shown in the right panel of Figs 2 and 3. We found a periodicity of $P_{\omega} = 148.2$ s with more than 99.99 per cent confidence only in the g band of Epoch 4, though we also note a nonstatistically significant signal at the same frequency in the r band of the same epoch (72.25 per cent confidence). In turn, we are not able to recover any signal from the LSP but, despite this, the g-band light curve from that same epoch exhibits short-term flares qualitatively similar to those observed in Epoch 4. We derive the analytical false alarm probability of our Epoch 4 g-band detection to be 1.16×10^{-6} ; the probability of detecting a signal of this significance in at least one of our 14 LSPs by chance (i.e. when there is no underlying signal) is 0.0016 per cent.

To determine the centre and 1σ uncertainty of the frequency detected in Epoch 4, and the coherence of this modulation, we performed a bootstrap analysis (e.g. Ivezić et al. 2014). We note that bootstrapping can also be used to reject sampling aliases (e.g.

Southworth et al. 2006), which may be present in the i-band LSP. From this analysis, we found peak frequencies of 6.73 ± 0.02 mHz (g band), 6.73 ± 0.02 mHz (r band), and 6.75 ± 0.02 mHz (i band). These frequencies correspond to periods of 148.5 ± 0.4 , 148.7 ± 0.4 , and 148.2 ± 0.5 s, respectively. To further test the coherence, we fit a Lorentzian to the Epoch 4 g-band periodogram (Belloni, Psaltis & van der Klis 2002) on top of our noise model (Vaughan 2005, top right panel in Fig. 3) and found a Q factor of 3422. The bootstrapped uncertainties and high Q factor are both indicative of a highly coherent signal.

To visualize the modulations identified in Epoch 4, we phasefolded these light curves on the peak frequencies inferred via our bootstrap analysis; we present these phase-folded light curves in Fig. 4, along with localized LSPs. Prominent modulations are only apparent in the g band, with a peak-to-peak amplitude of roughly 10 per cent (compared to an average 1σ white-noise amplitude of 2.6 per cent). The 3σ upper limits using the average white-noise amplitude for the Epochs 1, 2, 3, and 5 in g band are 4.8, 4.5, 14.5, and 10.5 per cent, respectively. For the LSPs, 99.99 per cent confidence thresholds were estimated by simulating 10 000 white-noise light curves for each band. Each simulated light curve had the same time sampling as the observed light curve, and fluxes were generated from the following Gaussian $f_i \sim \mathcal{N}(\bar{f}, \sigma_{f_i})$, where \bar{f} represents the mean flux of the observed light curve and σ_f represents the uncertainties on the observed flux values. As can be seen in Fig. 3, the periodograms of Epoch 4 are white-noise-dominated beyond 5 mHz, and so our estimated confidence thresholds are unlikely to be significantly biased in this frequency range.

To test the veracity of the signal, we have computed LSPs of the other stars as well as the background itself, in case the signal was produced by artefacts from the electron noise in the detectors. We have not found any significant signal in any of these. In Fig. 5, we present the LSP of the raw Epoch 4 *g*-band light curve for GOTO 0650 (top panel), along with the LSP of the corresponding local background (bottom panel). Fig. 5 shows a prominent peak in the periodogram of the raw flux at 6.7 mHz that is not seen in the

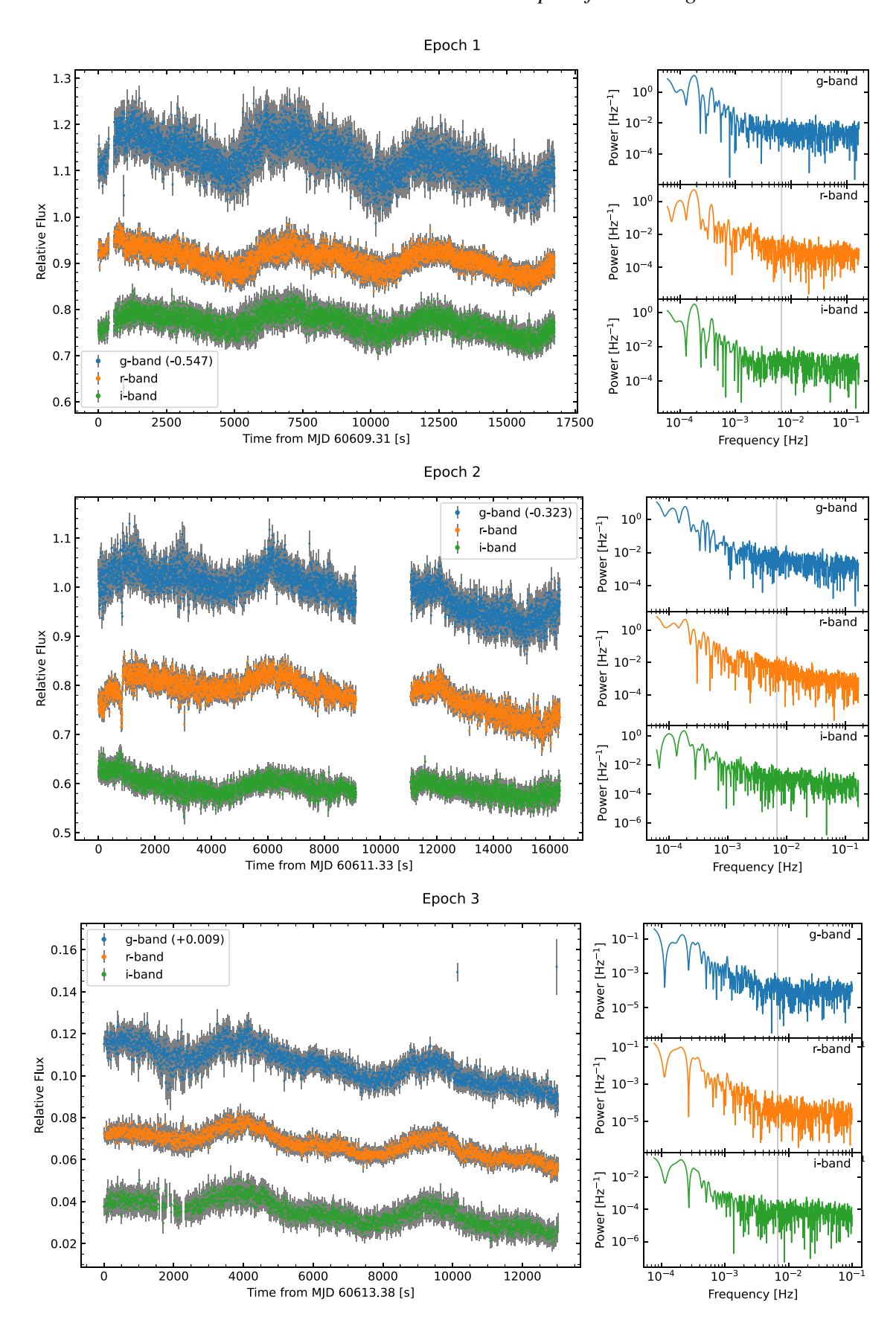


Figure 2. Relative light curves of all three cameras for Epochs 1–3 (left panels), along with their respective periodograms (right panels). The vertical shaded region in the power spectra indicates the frequency at which we detect a statistically significant signal in Epoch 4.

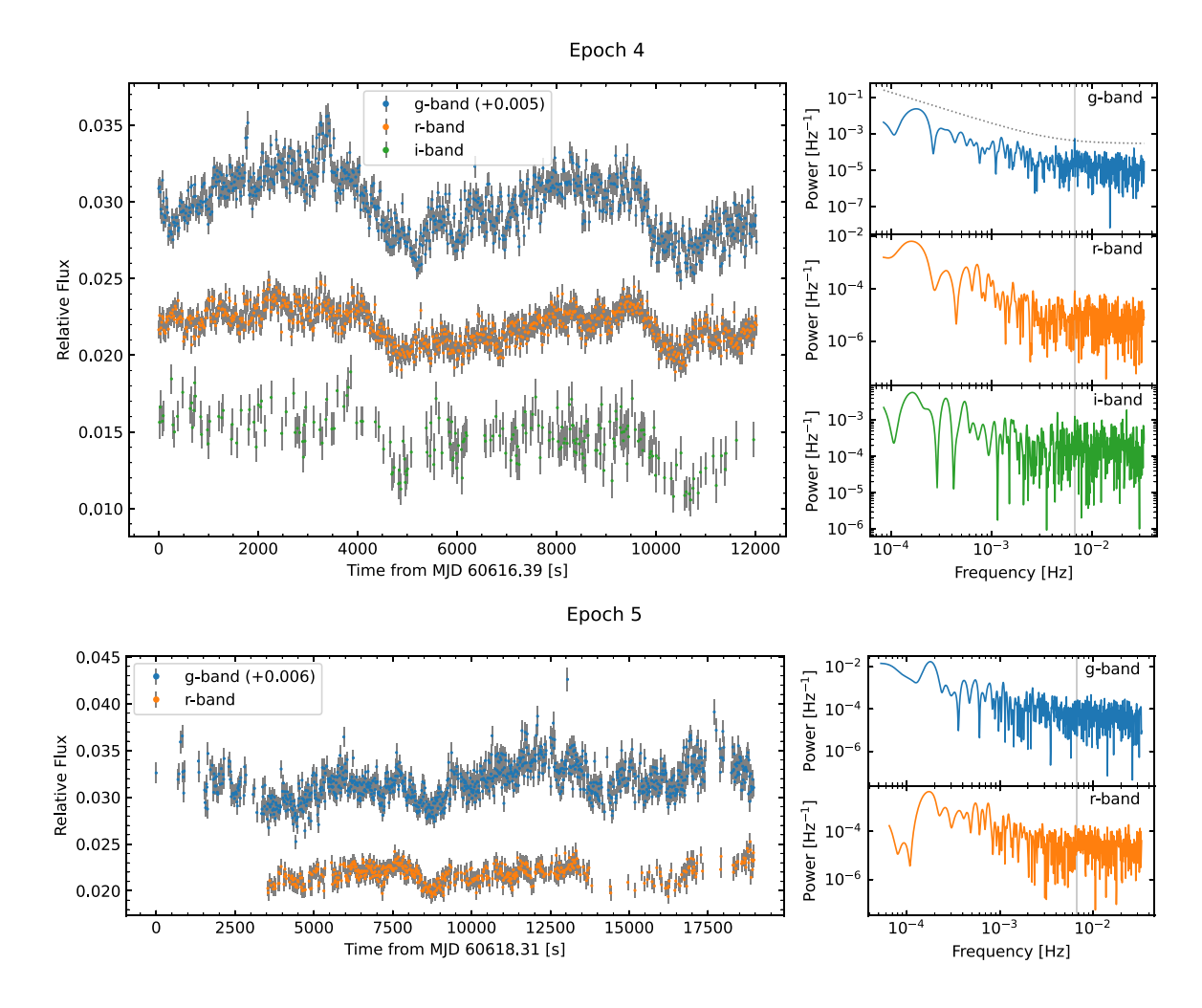


Figure 3. Same as Fig. 2 but for Epochs 4 and 5. For the *g*-band periodogram in Epoch 4, the 99.99 per cent confidence threshold is shown with a dotted line. The target was not detected in the *i* band during Epoch 5; therefore, only *g* and *r* bands are shown.

periodogram of the local background. This rules out the 6.7 mHz signal being attributable to our reference stars, or a result of some instrumental/systematic effect, and instead suggests that the signal is intrinsic to GOTO 0650.

4 DISCUSSION

In Section 3, we have unambiguously found evidence of a periodic signal with a period of 148.5 ± 0.4 s in Epoch 4 during the dip in-between the main outburst and the beginning of the rebrightenings/echo outburst of the newly discovered WZ Sge-type CV GOTO 0650. Unfortunately, the weather conditions did not allow us to recover the signal from Epoch 5, but the light curve from this night looks qualitatively similar. However, what is the origin of the 148.5 s signal observed in GOTO 0650? In this section, we will briefly explore the different physical mechanisms that can produce the observed signal.

This signal is present in g band with its amplitude decreasing towards longer wavelengths with a tentative detection in r band. This suggests a blue spectral component generating the detected signal, similar to the one seen in IPs. In addition to this, the frequency of the observed signal is comparable with the dominant signal of a typical IP. This makes the GOTO 0650 a WZ Sge-type IP the most obvious interpretation; none the less, we will consider other scenarios.

DN oscillations have been proposed to explain some variable periodicity in outbursting CVs (e.g. Marsh & Horne 1998; Woudt & Warner 2002); these are vertically extended regions of the disc or blobs being irradiated by the hot WD and boundary layer, which produce a signal corresponding to their Keplerian orbit. These signals are typically of the order of 10 s and evolve to slightly lower frequencies as the outburst evolves (up to 40 s). We do not detect any significant signal during the main outburst; therefore, we discard this scenario. The accretion-induced heating from the outburst makes non-radial pulsations of the WD also unlikely since the temperature of the WD should be too hot to be in the instability strip (cf. Clemens 1993; Toloza et al. 2016, but also see Szkody 2021), given its preoutburst temperature (Killestein et al. 2025). Finally, Veresvarska et al. (2024) proposed a precessing inner disc producing quasi periodic oscilations (QPOs) in a handful of CVs; however, these observed frequencies are typically one order of magnitude slower. Therefore, we conclude that GOTO 0650 is likely a WZ Sge IP; however, the stability of the signal would need to be tested once the system is back to quiescent levels.

Magnetism has been invoked to explain several properties of WZ Sge stars (see Section 1). WZ Sge itself is probably the most remarkable example of this class. This source exhibits fast optical, UV, and X-ray oscillations in quiescence (Robinson, Nather & Patterson 1978; Patterson 1980; Patterson et al. 1998; Skidmore et al.

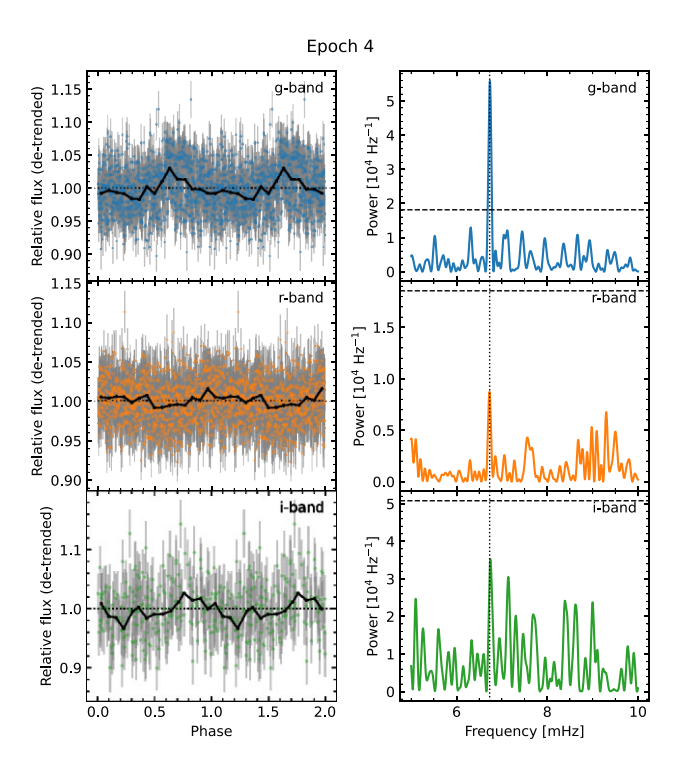


Figure 4. Left: Epoch 4 light curves folded on a period of 148.6 s (corresponding to 6.7 mHz). The black line represents the median values for the phase-binned folded light curve, the zero phase is arbitrary but common across bands. Right: Epoch 4 LSPs. In the LSPs, the dotted vertical line corresponds to a frequency of 6.7 mHz and the horizontal line represents the 99.99 per cent confidence threshold.

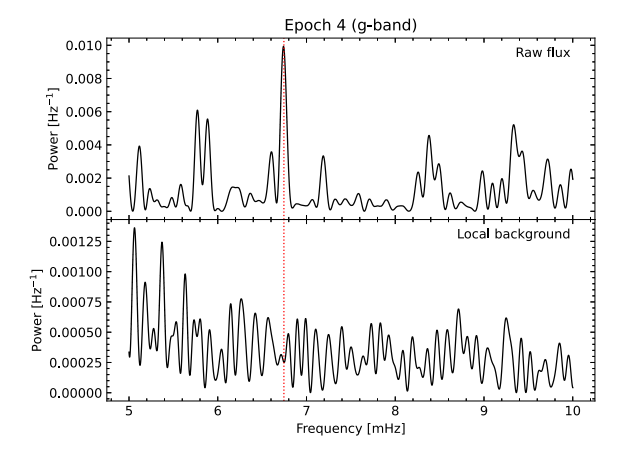


Figure 5. Top: LSP of GOTO 0650's raw flux from Epoch 4 in the g band. Bottom: LSP of the corresponding local background.

1999) around 27.87 s that have been associated with the spin period of the WD (Patterson et al. 1998). This signal is absent during outbursts owing to the combination of low magnetic field and/or low mass accretion rate from the donor; however, this interpretation has been challenged (cf. Knigge et al. 2002), leaving the origin of this signal an enduring enigma. CC Scl and ASASSN-18fk are also proposed to harbour a slowly spinning WD (Woudt et al. 2012; Pavlenko et al. 2019; Paice et al. 2024). Another remarkable example of an IP exhibiting superoutbursts is V455 And (Araujo-Betancor et al. 2005; Bloemen et al. 2013); this system exhibits a spin period of 67.6 s with the dominant signal in the power spectrum being twice the spin

period; however, it does not exhibit echo outbursts such as GOTO 0650 and WZ Sge. The time-scale of the signal observed in GOTO 0650 falls in-between that of CC Scl and V455 And, and the absence of the signal during outburst could be attributed to the combination of low magnetic field and/or mass transfer rate similar to what has been proposed for WZ Sge (Patterson et al. 1998). We then propose the observed signal as being produced by the spin period (or its first harmonic).

The data from Epoch 4 were obtained 2-3 d after the decline from the main outburst; therefore, the disc and magnetic torques would have been far from equilibrium during this epoch, making any estimation of the magnetic field highly uncertain. However, we can set a lower limit on the magnetic field as the source's magnetospheric radius must be larger than the WD radius. To do this, we need to estimate the mass accretion rate; for a canonical mass transfer rate of $\dot{M}_{\rm tr} \simeq 10^{-11} \, {\rm M}_{\odot} \, {\rm yr}^{-1}$ in WZ Sge stars (Knigge, Baraffe & Patterson 2011), typically expending ≥30 yr in quiescence between outbursts, and with an outburst duration of $\simeq 30$ d, we estimate the average mass accretion rate during the outburst to be $\langle \dot{M}_{\rm acc} \rangle \simeq 7 \times 10^{-9} \ {\rm M}_{\odot} \, {\rm yr}^{-1}$ in a conservative mass transfer scenario. Alternatively, we can obtain the peak mass accretion rate via the peak absolute magnitude $M_{\rm V}$ versus orbital period ($P_{\rm orb}$) and its relation with $\dot{M}_{\rm acc}$ (e.g. Warner 1987; Patterson 2011). For a source close to the period minimum (as GOTO 0650 is), we find the absolute magnitude at (superoutburst) peak to be $M_{\rm V} \simeq 5$, consistent with the value derived by Killestein et al. (2025). In turn, this value gives us an estimation of the mass accretion rate of $\dot{M}_{\rm acc} \simeq 2 \times 10^{-8} \ {\rm M_{\odot} \ yr^{-1}}$ (e.g. Warner 1987). We can therefore assume $\dot{M}_{\rm acc} \sim 10^{-8} \, {\rm M}_{\odot} \, {\rm yr}^{-1}$, a reasonable mass accretion rate during the main outburst of GOTO 0650. During Epoch 4, the source was two orders of magnitude fainter; therefore, assuming the bulk observed luminosity during this epoch being dominated by the accretion disc and given that this scales with the mass accretion rate ($L_{\rm acc} \propto \dot{M}_{\rm acc}$), we can adopt $\dot{M}_{\rm acc} \sim 10^{-10} \ {\rm M}_{\odot} \, {\rm yr}^{-1}$ during Epoch 4 as a reasonable approximate reference value for our calculations (acknowledging that it excludes corrections or additional spectral components, e.g. the hotspot). If the magnetosphere of the WD truncates the disc at the co-rotation radius, i.e. $r_{\rm M} = \xi r_{\rm A} = r_{\rm CO}$ (with $\xi \simeq 0.5$; e.g. Ghosh & Lamb 1979; Long, Romanova & Lovelace 2005), we can set a lower limit of the magnetic field, B, at which $r_{\rm M}=R_{\rm WD}$. For a typical 0.8 ${\rm M}_{\odot}$ WD in a CV (Zorotovic, Schreiber & Gänsicke 2011; Pala et al. 2017), this would give us a lower limit of $B \sim 2 \times 10^4$ G. This argument cannot be used for Epoch 3, since the disc is experiencing a rapid change, which will keep it even further from a stationary configuration. The same is not true for Epoch 2, thus allowing us to set an upper limit in the magnetic field strength. Assuming that the disc 'pushed' magnetosphere to the surface of the WD during the outburst, we can constrain the magnetic field to be $B \lesssim 4 \times 10^4 \text{ G}.$

In the hypothetical case of the disc and magnetic torques being in equilibrium during Epoch 4, we could estimate the magnetic field of the system; for $P_{\omega}=1$ and $2\times P_{\rm spin}$, this would correspond to a magnetic field of 5×10^4 and 10^5 G, respectively. The latter of these values would require an $\dot{M}_{\rm acc}\simeq 10^{-7}~{\rm M_{\odot}\,yr^{-1}}$ to push the magnetosphere down to the WD surface; this scenario not only goes against our constraints from above but it would make the system enter a super-Eddington wind regime (cf. Ma et al. 2013). We therefore suggest that P_{ω} may be the fundamental frequency of the spin period, and the WD's magnetic field would be of the order of $B\sim 10^4$ G. However, quiescent observations are required to test this hypothesis. If confirmed, GOTO 0650 would not only be another example of how magnetic fields can be dynamically important in highly evolved CVs

but also would bridge the gap between intermediate- and fast-rotating accreting WD systems.

ACKNOWLEDGEMENTS

We are grateful to the referee for their helpful feedback. We are grateful to many amateur astronomers for making their data publicly available in AAVSO. NCS and DLC acknowledge support from the Science and Technology Facilities Council (STFC) grant ST/X001121/1. ZAI, FMV, and DA acknowledge support from the STFC grants ST/V001000/1 and ST/X508767/1. IP acknowledges support from a Royal Society University Research Fellowship (URF\R1\231496). AC acknowledges support from the Royal Society Newton International Fellowship grant NF170803. This study is based upon observations carried out at the Observatorio Astronómico Nacional on the Sierra San Pedro Mártir (OAN-SPM), Baja California, México. We thank I. Zavala for maintaining the data acquisition software of OPTICAM.

DATA AVAILABILITY

The data underlying this letter are publicly available in AAVSO (ht tps://www.aavso.org) and ZTF (https://www.ztf.caltech.edu/ztf-public-releases.html). The remaining data will be shared on reasonable request to the corresponding author.

REFERENCES

Antonov N., Boeneker E. T., da Silva C. M., Dufoer S., Darlington G., Dubois F., Gaudenzi S., 2024, Observations from the AAVSO International Database, https://www.aavso.org

Araujo-Betancor S. et al., 2005, A&A, 430, 629

Bellm E. C. et al., 2019a, PASP, 131, 018002

Bellm E. C. et al., 2019b, PASP, 131, 068003

Belloni T., Psaltis D., van der Klis M., 2002, ApJ, 572, 392

Bhattacharya S., Bhattacharyya S., 2024, Astron. Telegram, 16866, 1

Bloemen S., Steeghs D., De Smedt K., Vos J., Gänsicke B. T., Marsh T. R., Rodriguez-Gil P., 2013, MNRAS, 429, 3433

Bradley L. et al., 2024, astropy/photutils: 1.13.0, Zenodo, European Organization for Nuclear Research (CERN)

Campana S., Stella L., Mereghetti S., de Martino D., 2018, A&A, 610, A46

Castro A. et al., 2019, Rev. Mex. Astron. Astrofis., 55, 363

Castro A. et al., 2024, New Astron., 112, 102262

Castro Segura N. et al., 2021, MNRAS, 501, 1951

Clemens J. C., 1993, Balt. Astron., 2, 407

Dyer M. J. et al., 2024, in Marshall H. K., Spyromilio J., Usuda T., eds, Proc. SPIE Conf. Ser. Vol. 13094, Ground-based and Airborne Telescopes X. eid. 130941X, Society of Photo-Optical Instrumentation Engineers (SPIE) Conference Series, p.130941X

Eracleous M., Horne K., 1996, ApJ, 471, 427

Georganti M., Knigge C., Castro Segura N., Long K. S., 2022, MNRAS, 511, 5385

Ghosh P., Lamb F. K., 1979, ApJ, 234, 296

Hameury J. M., 2020, Adv. Space Res., 66, 1004

Ivezić Ž., Connolly A. J., VanderPlas J. T., Gray A., 2014, Statistics, Data Mining, and Machine Learning in Astronomy: A Practical Python Guide for the Analysis of Survey Data. Princeton Univ. Press, Princeton, NJ

```
Kato T., 2015, PASJ, 67, 108
```

Killestein T. et al., 2024a, Astron. Telegram, 16842, 1

Killestein T. et al., 2024b, Astron. Telegram, 16858, 1

Killestein T. L. et al., 2025, preprint (arXiv:2501.11524)

Kimura M. et al., 2018, PASJ, 70, 47

Kimura M., Osaki Y., Kato T., Mineshige S., 2020, PASJ, 72, 22

Knigge C., Baraffe I., Patterson J., 2011, ApJS, 194, 28

Knigge C., Hynes R. I., Steeghs D., Long K. S., Araujo-Betancor S., Marsh T. R., 2002, ApJ, 580, L151

Lasota J.-P., 2016, in Bambi C., ed., Astrophysics and Space Science Library, Vol. 440, Astrophysics of Black Holes. Springer-Verlag, Berlin, p. 1

Littlefield C., Scaringi S., Garnavich P., Szkody P., Kennedy M. R., Iłkiewicz K., Mason P. A., 2021, AJ, 162, 49

Lomb N. R., 1976, Ap&SS, 39, 447

Long M., Romanova M. M., Lovelace R. V. E., 2005, ApJ, 634, 1214

Ma X., Chen X., Chen H.-l., Denissenkov P. A., Han Z., 2013, ApJ, 778, L32 Marsh T. R., Horne K., 1998, MNRAS, 299, 921

McCully C. et al., 2018, astropy/astroscrappy: v1.0.5 Zenodo Release.

Zenodo, European Organization for Nuclear Research (CERN) Naylor T., 1998, MNRAS, 296, 339

Paice J. A. et al., 2024, MNRAS, 531, L82

Pala A. F. et al., 2017, MNRAS, 466, 2855

Patterson J. et al., 2005, PASP, 117, 1204

Patterson J., 1980, ApJ, 241, 235

Patterson J., 2011, MNRAS, 411, 2695

Patterson J., Richman H., Kemp J., Mukai K., 1998, PASP, 110, 403

Pavlenko E. et al., 2019, Contrib. Astron. Obs. Skalnate Pleso, 49, 204

Robinson E. L., Nather R. E., Patterson J., 1978, ApJ, 219, 168

Scargle J. D., 1982, ApJ, 263, 835

Skidmore W., Welsh W. F., Wood J. H., Catalán M. S., Horne K., 1999, MNRAS, 310, 750

Smak J., 1993, Acta Astron., 43, 101

Smak J., 2009, Acta Astron., 59, 121

Southworth J., Gänsicke B. T., Marsh T. R., de Martino D., Hakala P., Littlefair S., Rodríguez-Gil P., Szkody P., 2006, MNRAS, 373, 687

Steeghs D. et al., 2022, MNRAS, 511, 2405

Szkody P., 2021, Front. Astron. Space Sci., 8, 184

Tampo Y., 2024, GOTO065054.49+593624.51: Type-E Rebrightening WZ Sge Star? VSNET, Department of Astronomy, Kyoto, http://ooruri.kusastro.kyoto-u.ac.jp/mailman3/hyperkitty/list/vsnet-a lert@ooruri.kusastro.kyoto-u.ac.jp/thread/TWMZC3AKMJHBRPUB NRLYHGTKDCJKITDO/

Toloza O. et al., 2016, MNRAS, 459, 3929

van Dokkum P. G., 2001, PASP, 113, 1420

VanderPlas J. T., 2018, ApJS, 236, 16

Vaughan S., 2005, A&A, 431, 391

Vaughan S., Edelson R., Warwick R. S., Uttley P., 2003, MNRAS, 345, 1271

Veresvarska M. et al., 2024, MNRAS, 534, 3087

Warner B., 1987, MNRAS, 227, 23

Warner B., 1995, Cataclysmic Variable Stars, Vol. 28. Cambridge University Press (Cambridge Astrophysics), Cambridge

Woudt P. A. et al., 2012, MNRAS, 427, 1004

Woudt P. A., Warner B., 2002, MNRAS, 333, 411

Zorotovic M., Schreiber M. R., Gänsicke B. T., 2011, A&A, 536, A42

This paper has been typeset from a TEX/LATEX file prepared by the author.